

Multi-strain disease dynamics on a metapopulation network

Matthew Michalska-Smith¹ and craft²

¹University of Minnesota

²Affiliation not available

June 8, 2019

1 Abstract

2 Target Journal(s): Plos CB, Ecological Modelling, PRE, JTB, Oikos

3 Aims

4 1. develop easy to use (R package?) extension to MANTIS framework to consider a network of interconnected
5 populations

6 2. demonstrate some different dynamics possible using this framework and different parameterizations (emphasis on
7 network structure)

8 - directed movement

9 - classic network structures (Erdős–Rényi, small world, “realistic” spatially structured)

10 - incorporating local transmission as well as movements

11 3. explore differences in application, e.g. deterministic-static, deterministic-dynamic, stochastic-static, etc.

12 Many of the most impactful diseases that affect humans, livestock, and wildlife have clusters in their population-
13 genetic variability that we classify as strains. Importantly, host immunity to one of these strains is neither inde-
14 pendent from nor equivalent to immunity to related strains. This partial cross-protective immunity affects disease
15 dynamics across the population as a whole and can dramatically influence intervention strategies. While the study
16 of multi-strain diseases goes back decades, this work has not yet been generalized to a loosely connected collection of
17 subpopulations, i.e. a metapopulation. Starting from the strain theory of host-pathogen systems proposed by [Gupta](#)

18 (1998), we simulate multi-strain disease dynamics on a network of interconnected populations, characterizing the
19 effects of parameterization and network structures on these dynamics. We find that dynamics propagate through
20 the metapopulation network, even if parameters vary between populations. Moreover, in chains of connected po-
21 pulations experiencing cyclical dynamics, the movement of (partially) immune individuals dampens the dynamics
22 of populations further along the chain. This work serves as an important first step in extending prior results on
23 multi-strain diseases to a generalized population structure. This extension is particularly apt in the case of livestock
24 production, where a system of mostly isolated populations (farms) is connected through the forced movement of
25 individuals.

26 1 Introduction

27 Many of the most impactful infectious diseases that affect humans, livestock, and wildlife have
28 clusters in their population-genetic variability that we classify as strains. Such variation in pathogen
29 genotype often leads to differences in phenotype as well, importantly affecting the efficacy of host
30 immune defenses. While the human immune system is usually capable of preventing re-infection
31 with a pathogen to which it has been previously exposed, sufficient evolution on the part of the
32 pathogen can lead to reduced recognition by the host. In some cases, this change is not sufficient
33 to completely avoid recognition, however, leading to an immune response that is neither as strong
34 as would be in the case of re-exposure to the same strain, nor as weak as in the case of exposure to
35 a novel pathogen. This partial cross-protective immunity can lead to reduced transmission as well,
36 affecting disease dynamics across the population.

37 Malaria, Cholera, Human Papillomavirus Virus, Dengue, Porcine Reproductive and Respiratory
38 Syndrome, Brucellosis, *etc.* have strain structure, but differ in both the number of strains and the
39 level of cross-protective immunity afforded by past exposure to similar strains. Perhaps the most
40 well-studied example is that of Influenza (flu), a viral respiratory tract infection that counts hu-
41 mans among its many potential hosts and has substantial economic and public health consequences
42 worldwide ([Molinari et al., 2007](#); [Fan et al., 2016](#); [Peasah et al., 2013](#)).

43 While the study of multi-strain diseases goes back decades, this work has not yet been generalized
44 to a loosely connected collection of sub-populations, *i.e.* a metapopulation. Initially introduced
45 through the concepts of island biogeography, this idea can be generalized to a variety of systems,
46 including human movement between cities, livestock transport between farms, and populations
47 living in fragmented natural habitats. In each case, there exist relatively high-density areas which
48 are connected to one another through a network of individuals' movement. This framework allows the
49 application of network analyses that can characterize patterns of connection within the population
50 as a whole.

51 Historically, metapopulation studies have been divided into two main camps: those that model

52 within-patch dynamics and “cell occupancy” models in which only the presence or absence of a given
53 species within a patch is recorded (Taylor, 1988), with the latter receiving much more theoretical
54 attention. Importantly, this latter case rests on an assumption of temporal separation in which local
55 dynamics occur on a timescale that can be treated as instantaneous relative to that of the between-
56 patch dynamics (Hanski, 1994). When considering diseases in systems with relatively high migration
57 rates, however, this assumption rarely holds and the presence-absence approach can significantly
58 affect model accuracy, especially when individual disease status might affect migration rates.

59 Here, we build on the strain theory of host-pathogen systems proposed by Gupta (1998), considering
60 the case where a collection of populations undergoing local dynamics are furthermore interconnected
61 through the movement of individuals between populations. We simulate disease dynamics on this
62 system, characterizing the effects of parameterization and network structures on these dynamics.
63 This work is divided into three sections: first, we explore the simple case of interconnected popu-
64 lations with identical parameterizations. Second, we consider the case in which parameters differ
65 between populations. Finally, we explore the case of a larger network of connected populations,
66 looking at the role of network structure on key measures of disease progression.

67 2 Methods

68 2.1 Model framework for one population

69 We work from a system of ordinary differential equations detailing the proportion of a population
70 in classes based on current and past exposure to different strains of a pathogen. We signify a strain
71 $i = \{x_1, x_2, \dots, x_n\}$ as a set of n loci, each of which can take on a finite number of alleles. For
72 instance, a pathogen with two loci (a and b) and two alleles at each loci has a total of four potential
73 strains: $\{a_1, b_1\}$, $\{a_1, b_2\}$, $\{a_2, b_1\}$, $\{a_2, b_2\}$. Importantly, in this model framework, the number of
74 strains is fixed and finite. While strains may go extinct over time, there is no process for the
75 generation of new strains or to re-introduce strains that had previously gone extinct (Gupta, 1998,
76 but see).

77 The model consists of sets of three nested equations (one set for each strain): w , z , and y , where
78 each set consists of as many equations as there are strains. w_i represents the proportion of the
79 population which has been exposed to a strain j of the pathogen, where strain j has at least one
80 allele in common with strain i , *i.e.*, $j \cap i \neq \emptyset$. z_i represents the proportion of the population that
81 has been exposed to strain i itself. Finally, y_i represents that proportion of the population currently
82 infected with strain i (and thus capable of infecting others). Thus, the proportion of the population
83 in y_i is also in z_i and the proportion of the population in z_i is also in w_i , and $y_i \leq z_i \leq w_i$. The
84 y class is analogous to the I class in standard SI , SIR , *etc.* single-strain frameworks, while w and
85 z are composed of combinations of I and R classes. The susceptible population is not modeled
86 explicitly in this framework.

87 These equations have the form:

$$\begin{aligned}
\frac{dy_i}{dt} &= \beta ((1 - w_i) + (1 - \gamma)(w_i - z_i)) y_i - \sigma y_i - \mu y_i \\
\frac{dz_i}{dt} &= \beta (1 - z_i) y_i - \mu z_i \\
\frac{dw_i}{dt} &= \beta (1 - w_i) \sum_{j \ni j \cap i \neq \emptyset} y_j - \mu w_i
\end{aligned} \tag{1}$$

88 Where, as above, we denote strains as subscripts and in the equation for w_i we sum over all strains
89 j which share at least one allele with the focal strain i . β , σ , and μ are the infection, recovery, and
90 death rates, respectively. γ is an indicator of the level of cross-protective immunity gained by prior
91 exposure to alleles in the target strain. Note that while we depict only one value per demographic
92 parameter (*i.e.*, all strains are functionally equivalent) for notational clarity, these values could also
93 vary by strain (*e.g.*, β_i) in this framework.

94 Note that immunity in this framework is non-waning: exposure to a strain yields consistent protecti-
95 on from future infection over the lifespan of the individual. The level of this infection is dichotomous:
96 with respect to the same strain, it is complete protection, with respect to any strain sharing at least
97 one allele, it modifies infection risk according to the parameter γ . Importantly, we also do not distin-
98 guish between loci, assuming that sharing an allele at any locus is functionally identical to sharing

99 an allele at any other locus.

100 2.2 Extensions to consider more than one population

101 Following [Xiao et al. \(2011\)](#), we model movement between populations using a dispersal matrix
102 $\Delta = A - E$, where A is the weighted adjacency matrix indicating the proportion of individuals
103 moving from from patch i (row) to patch j (column) and E is a diagonal matrix representing
104 emigration, where each entry $E_{jj} = \sum_{i=1}^n A_{ij}$ where n is the number of patches. Thus, the whole
105 system can be depicted by a set of three equations for each strain i in each patch k :

$$\begin{aligned}\frac{dy_{i,k}}{dt} &= \beta((1 - w_{i,k}) + (1 - \gamma)(w_{i,k} - z_{i,k}))y_{i,k} - \sigma y_{i,k} - \mu y_{i,k} + \sum_l \Delta_{kl} y_{j,l} \\ \frac{dz_{i,k}}{dt} &= \beta(1 - z_{i,k})y_{i,k} - \mu z_{i,k} + \sum_l \Delta_{kl} z_{j,l} \\ \frac{dw_{i,k}}{dt} &= \beta(1 - w_{i,k}) \sum_{j \ni j \cap i \neq \emptyset} y_{j,k} - \mu w_{i,k} + \sum_l \Delta_{kl} w_{j,l}\end{aligned}\tag{2}$$

106 Where each equation is now additionally indexed according to population. While in principle the
107 elements of Δ can take any value $[0, 1]$, signifying a movement of between 0 and 100% of individuals,
108 for simplicity we use a constant value of $\delta = 0.1$ for the strength of each movement. **TODO:**
109 **Sensitivity to this value is explored in the Supplementary Information.**

110 Note that this formulation assumes uniform sampling for migration between populations. One might
111 imagine cases in which currently infectious individuals are less likely to migrate than those who have
112 recovered and now have immunity. **TODO:** We explore this variation in migration structure in the
113 **Supplementary Information.**

114 This framework can be applied to a metapopulation of arbitrary size and complexity. Fundamentally,
115 the dynamics of each population will be governed by a set of three equations per disease strain,
116 and these equations are interlinked within a population by partial, cross-protective immunity, and
117 between populations through a network specifying movement of individuals between patches. Thus,
118 the total number of differential equations for any given system will be 3 x the number of strains x

119 the number of patches in the metapopulation.

120 2.3 Simulation Prodedure

121 All simulations were carried out in Julia (Bezanson et al., 2017), with graphics produced using the
122 ggplot package (Wickham, 2016) in R (R Core Team, 2019). In addressing the first two objectives
123 mentioned above, we fix the values of all variables other than γ (the degree of cross-protective
124 immunity) and Δ (the network of movement information). The former is varied to demonstrate the
125 variety of dynamics obtainable in this modeling framework (as in Gupta (1998)), while the latter
126 varies the number and interconnections of the network patches.

127 For each of the following simulations, we assume that there is no mortality, but add movement out
128 of each sink population to balance in- and out-flows in the system. This simplification does not
129 qualitatively change the dynamics of the system.

130 For Figure 1, we use a movement network described by a chain of populations, *i.e.* $A \rightarrow B \rightarrow C \rightarrow D$

131 or $\Delta = \begin{bmatrix} -\delta & \text{amp}; \delta & \text{amp}; 0 & \text{amp}; 0 \\ 0 & \text{amp}; -\delta & \text{amp}; \delta & \text{amp}; 0 \\ 0 & \text{amp}; 0 & \text{amp}; -\delta & \text{amp}; \delta \\ 0 & \text{amp}; 0 & \text{amp}; 0 & \text{amp}; -\delta \end{bmatrix}$, where $\delta = 0.1$.

132 For figure 2, we restrict our consideration to a system of two patches, identical in all respects other
133 than the parameter γ , which is set to either induce a steady state of coexistence ($\gamma = 0.25$ in popula-
134 tion A) or cyclical coexistence ($\gamma = 0.75$ in population B). We then display three potential patterns
135 of connection: $A \rightarrow B$ (right column), $B \rightarrow A$ (left column), and the case of no migration between

136 patches (middle column). Specifically, we set $\Delta = \begin{bmatrix} -\delta & \text{amp}; \delta \\ 0 & \text{amp}; -\delta \end{bmatrix}$, $\Delta = \begin{bmatrix} -\delta & \text{amp}; 0 \\ \delta & \text{amp}; -\delta \end{bmatrix}$, and $\Delta =$

137 $\begin{bmatrix} -\delta & \text{amp}; 0 \\ 0 & \text{amp}; -\delta \end{bmatrix}$, respectively.

138 Finally, for XXXXX, we consider a system of three populations: $A \rightarrow C \leftarrow B$, or $\Delta = \begin{bmatrix} -\delta & \text{amp}; 0 & \text{amp}; \delta \\ 0 & \text{amp}; -\delta & \text{amp}; \delta \\ 0 & \text{amp}; 0 & \text{amp}; -\delta \end{bmatrix}$, wh
139 populations A and C have $\gamma = 0.25$, but population B has $\gamma = 0.75$.

140 3 Results

141 3.1 Dynamics are dampened along chains in the metapopulation network

142 We find that even when all populations share the same parameterizations and initial conditions,
143 that populations further along network chains have dampened oscillatory dynamics compared to
144 those they would exhibit in isolation (Figure 1). This is likely due to the movement of (partially) im-
145 mune individuals between the populations, increasing the proportion of specific and cross-reactively
146 immune individuals in populations further along the chain. While infectious individuals move at an
147 equal rate, the proportion of the population that is currently infectious at any given time is much
148 smaller than the proportion with immunity.

149 3.2 Dynamics propagate through metapopulation networks

150 We find that in the case of a simple chain of populations, the dynamics of sink populations can
151 be overridden by the dynamics of source populations (Figure 2). Interestingly, this is true both
152 of cyclical dynamics overruling stable dynamics and *vice versa*. In the case of multiple source
153 populations, cycles tend to dominate over stable dynamics. Importantly, this migration can allow
154 for strain coexistence even in populations where the disease parameters would suggest extinction of
155 one or more strains.

156 3.3 There exists a dynamics hierarchy

157 The issue of dynamics propagation gets more complicated when there are multiple, varying source
158 populations for a given sink population. We find that there is a hierarchy of dynamics in their
159 propagation through the network: cyclical dynamics overpower steady states and chaos overpowers

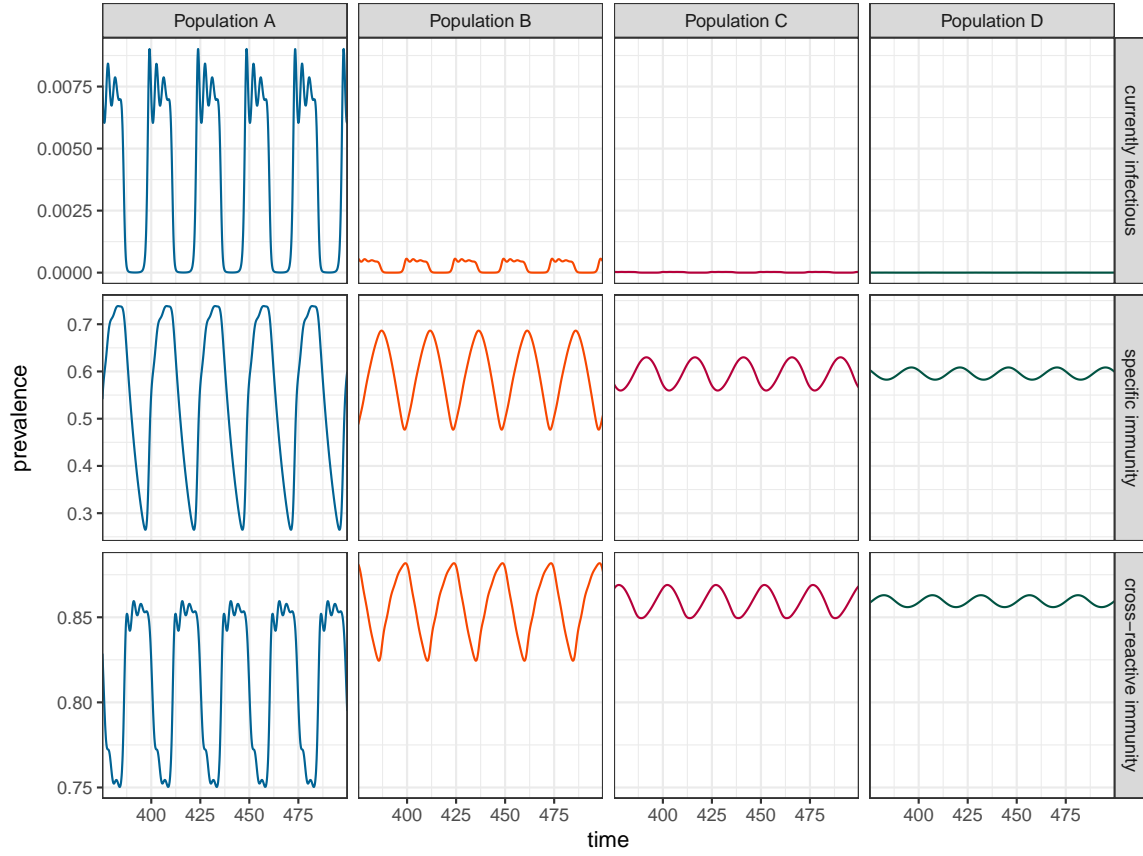


Figure 1: Connecting multiple populations with the same dynamics results in dampened cycles in populations further down the chain. Here, populations are connected such that $A \rightarrow B \rightarrow C \rightarrow D$. Importantly, the mean level of immunity (cross-reactive and specific) increases in each sequential population, while the mean level of currently infectious decreases. All populations have parameters $\beta = 40$, $\sigma = 10$, $\mu = 0$, $\delta = 0.1$, $\gamma = 0.75$.

160 cycles, regardless of any imbalance in the relative contributions of the sources. Put another way,
 161 if just one of many source populations (or a small proportion of the total movement) has cyclical
 162 dynamics, the sink population will also have cyclical dynamics.

163 Note that even though this parameterization would lead to steady state dynamics in population C
 164 in the absence of migration, we see cyclical dynamics being inherited from population

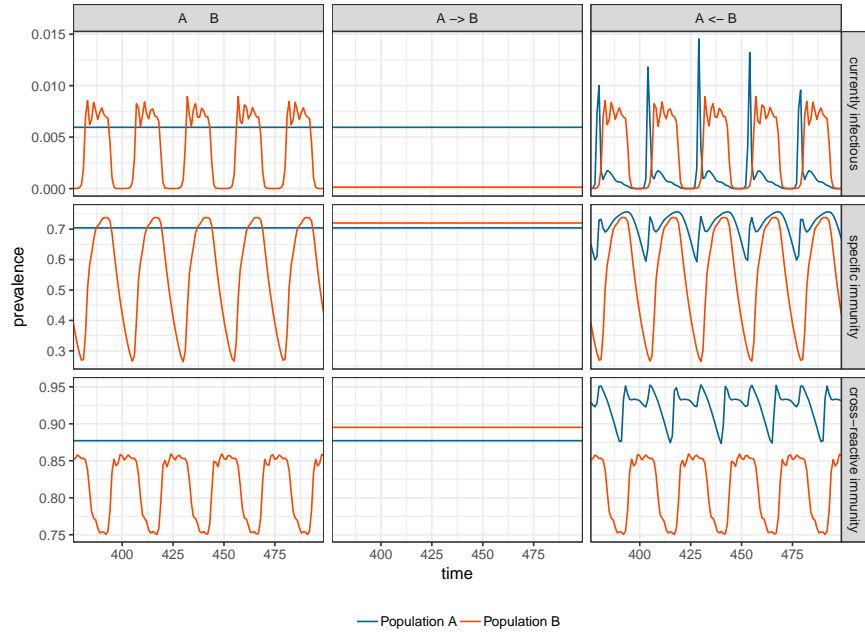


Figure 2: The effect of linking populations with different model parameterizations. While in isolation (center column), population A has steady-state dynamics and population B has cyclical dynamics, when the two populations are linked by migration, the sink population inherits the dynamics of the source population (left and right columns). This is true regardless of the direction of the movement. Populations have parameters $\beta = 40$, $\sigma = 10$, $\mu = 0$, $\delta = 0.1$ in common and $\gamma = 0.25$, 0.75 respectively.

165 4 Discussion

166 4.1 Moving away from densities

167 This modelling framework does not model the disease state of individuals directly, but rather fo-
 168 cuses on the proportion of the population that is/has been infected with each possible disease strain.
 169 Importantly, empirical movement data is usually not in the form of proportions, but rather num-
 170 bers of individuals moving (often at a specific time as well). To fully model the disease status of
 171 each individual in the metapopulation would result in an explosion of total number of differential
 172 equations due to the factorial expansion of possible disease histories.

173 Alternatively, one could develop an individual based model...

174 **4.2 Generalizing to larger network structures**

175 **4.3 Dynamic & stochastic movement networks**

176 **5 Supplementary Information**

177 **5.1 Additional Figures (?)**

178 1. explanatory figures

179 (a) basic model structure figure (perhaps analogous to figures in [Lourenço et al. \(2015\)](#) or
180 [Wikramaratna et al. \(2013\)](#))

181 (b) network structure differences (figure or table)

182 2. results figures

183 (a) figure of dynamics on “realistic” network structure

184 3. supplementary figures

185 (a) repeat results figures with different “applications” (see above)

186 **5.2 Key assumptions**

187 1. Individuals do not die, but are transferred off-site (?)

188 2. all individuals equally likely to migrate

189 **References**

190 Jeff Bezanson, Alan Edelman, Stefan Karpinski, and Viral B. Shah. Julia: A Fresh Approach to
191 Numerical Computing. *SIAM Review*, 59(1):65–98, jan 2017. doi: 10.1137/141000671. URL
192 <https://doi.org/10.1137%2F141000671>.

193 Victoria Fan, Dean Jamison, and Lawrence Summers. The Inclusive Cost of Pandemic Influenza
194 Risk. Technical report, mar 2016. URL <https://doi.org/10.3386/2Fw22137>.

195 S. Gupta. Chaos Persistence, and Evolution of Strain Structure in Antigenically Diverse Infectious
196 Agents. *Science*, 280(5365):912–915, may 1998. doi: 10.1126/science.280.5365.912. URL <https://doi.org/10.1126/2Fscience.280.5365.912>.

197

198 Ilkka Hanski. A Practical Model of Metapopulation Dynamics. *The Journal of Animal Ecology*, 63
199 (1):151, jan 1994. doi: 10.2307/5591. URL <https://doi.org/10.2307/2F5591>.

200 José Lourenço, Paul S Wikramaratna, and Sunetra Gupta. MANTIS: an R package that simulates
201 multilocus models of pathogen evolution. *BMC Bioinformatics*, 16(1), may 2015. doi: 10.1186/
202 s12859-015-0598-9. URL <https://doi.org/10.1186/2Fs12859-015-0598-9>.

203 Noelle-Angelique M. Molinari, Ismael R. Ortega-Sanchez, Mark L. Messonnier, William W. Thomp-
204 son, Pascale M. Wortley, Eric Weintraub, and Carolyn B. Bridges. The annual impact of seasonal
205 influenza in the US: Measuring disease burden and costs. *Vaccine*, 25(27):5086–5096, jun 2007. doi:
206 10.1016/j.vaccine.2007.03.046. URL <https://doi.org/10.1016/2Fj.vaccine.2007.03.046>.

207 Samuel K. Peasah, Eduardo Azziz-Baumgartner, Joseph Breese, Martin I. Meltzer, and Marc-Alain
208 Widdowson. Influenza cost and cost-effectiveness studies globally – A review. *Vaccine*, 31(46):
209 5339–5348, nov 2013. doi: 10.1016/j.vaccine.2013.09.013. URL <https://doi.org/10.1016/2Fj.vaccine.2013.09.013>.

210

211 R Core Team. *R: A Language and Environment for Statistical Computing*. R Foundation for
212 Statistical Computing, Vienna, Austria, 2019. URL <https://www.R-project.org/>.

213 Andrew D. Taylor. Large-scale spatial structure and population dynamics in arthropod predator-
214 prey systems. *Annales Zoologici Fennici*, pages 63–74, 1988.

215 Hadley Wickham. *ggplot2: Elegant Graphics for Data Analysis*. Springer-Verlag New York, 2016.
216 ISBN 978-3-319-24277-4. URL <https://ggplot2.tidyverse.org>.

217 P. S. Wikramaratna, M. Sandeman, M. Recker, and S. Gupta. The antigenic evolution of influenza:

218 drift or thrift? *Philosophical Transactions of the Royal Society B: Biological Sciences*, 368(1614):
219 20120200–20120200, feb 2013. doi: 10.1098/rstb.2012.0200. URL [https://doi.org/10.1098/
220 2Frstb.2012.0200](https://doi.org/10.1098/2Frstb.2012.0200).

221 Y. Xiao, Y. Zhou, and S. Tang. Modelling disease spread in dispersal networks at two levels.
222 *Mathematical Medicine and Biology*, 28(3):227–244, September 2011. doi: 10.1093/imammb/
223 dqg007. URL [https://doi.org/10.1093/imammb/
dqg007](https://doi.org/10.1093/imammb/dqg007).